This is a peer-reviewed, accepted author manuscript of the following research article: Ewe, W. E., Sopian, K., Mohanraj, M., Fudholi, A., Asim, N., & Ibrahim, A. (2023). Exergetic performance of jet impingement bifacial photovoltaic-thermal solar air collector with different packing factors and jet distributions. *Heat Transfer Engineering*. https://doi.org/10.1080/01457632.2023.2227807

Exergetic performance of jet impingement bifacial photovoltaic-thermal (PVT) solar air collector with different packing factors and jet distributions

Win Eng Ewe[a], Kamaruzzaman Sopian[a,*], M. Mohanraj[b], Ahmad Fudholi[a], Nilofar Asim[a], Adnan Ibrahim[a]

[a] Solar Energy Research Institute, Universiti Kebangsaan Malaysia, 43600 Bangi, Malaysia.

[b]Hindusthan College of Engineering and Technology, Coimbatoire Coimbatore-641032, Tamilnadu, India.

*Address correspondence to Prof. Kamaruzzaman Sopian, Solar Energy Research Institute (SERI), Level G, Research Complex, Universiti Kebangsaan Malaysia, 43600 Bangi, Selangor, MALAYSIA. E-mail: ksopian@ukm.edu.my. Tel: (+60) 3-89118022

*Corresponding author.
E-mail addressess: p97455@siswa.ukm.edu.my (W.E. Ewe)

Abstract

Jet impingement is a promising cooling mechanism to increase the rate of heat transfer in solar air collector. However, the effects of impinging air jet on the exergetic performance of a bifacial photovoltaic-thermal with different packing factors are entirely unclear. In this research, a jet impingement bifacial photovoltaic-thermal solar air collector was developed and its exergetic performance was assessed. Jet plate reflectors with different geometric configurations are proposed to enhance the cooling and light absorption at the rear part of the bifacial photovoltaic module. Additionally, the link between exergetic performance and each variable's design and operational characteristics was examined through indoor experiments. The results showed that the maximum exergy efficiency of the bifacial photovoltaic-thermal with packing factor of 0.66 and 36-hole jet plate reflector has 11.88 % under solar irradiance of 900 W/m^2, and mass flow rate of 0.025 kg/s. The maximum exergy input, exergy destruction and improvement potential of the proposed system are 402.81 W, 345.62 W and 304.78 W, respectively.

Introduction

Solar air collectors with glazed jet impingement technology were created for the first time in [1], which shown that by including a jet air impingement mechanism, it is possible to enhance the optimum thermal output of a conventional solar air collector (SAC) by 26.5%. This unglazed SAC with jet impingement was investigated and had shown 21% higher in thermal efficiency, compared to flat plate SAC [2]. Besides, Chauhan and Thakur [3] have examined the link between the friction factor and the Nusselt number in the context of jet plate SAC in order to determine the optimum operating parameters and geometric characteristics on a jet plate. The results showed that the friction factor and heat transfer rate were enhanced by a factor of 3.5 and 2.6, respectively. Another research done by the same scientists [4] proposed that the ideal jet plate parameters were calculated theoretically by utilizing the correlations to calculate the greatest thermohydraulic efficiency. Following that, the optimum design configuration has determined for spanwise pitch, jet diameter, and streamwise pitch ratios of 0.065, 0.435, and 0.865, respectively [5]. In a similar study, the thermal efficiency of a flat plate SAC and perforated plate with low porosity was investigated [6]. The results suggest that the perforated plate with minimal porosity has 23% improved thermal efficiency than the flat plate. It has been demonstrated that a dual-channel SAC with jet plate which integrated ribs on absorber plate has 21.2 % higher in thermal efficiency and 22.4 % higher in exergy efficiency than a single channel SAC with jet plate [7]. Hence, it was proven that jet impingement increases the heat transfer and thermal performance of solar air collectors.

Photovoltaic-thermal (PVT) systems convert solar energy to heat and electricity simultaneously. Comparing to stand-alone photovoltaic (PV) or solar thermal systems, a higher efficiency can be obtained by PVT systems due to higher energy density [8]. However, when the temperature rises, the solar panel's performance decreases [9]. As a result, various cooling techniques have been developed to enhance the PV power produced avid reducing the panel temperature [10]. An analytical model was used to quantify the jet impinging PVT's performance, and reported with a total efficiency of 54% [11]. Additional research in [12] indicated that the double pass bifacial PVT systems had optimum total energy efficiency of 67%. By impinging Si-C nanofluids on a jet array, it was proven that [13], a PVT solar collector's total efficiency was improved. Experiments had achieved electrical, thermal, and total efficiencies of 12.8 %, 85 %, and 97.8 %, correspondingly. Similar authors did similar investigation by replacing the coolant with water and the system achieved 81% of total energy efficiency [14]. In [15], PVT -CPC was introduced with the water jet. Compared with a conventional PV module, water jet cooling increases the electrical and thermal performance as well as the output power by 7%, 81% and 31%, respectively. In [16], PV modules with water jet cooling were presented. It was found that the minimum distance of the spray jet to the PV module and the jet diameter at the maximum number of jets contributed to an optimum temperature and power generation of 33.7 ℃ and 8.61 W, respectively. Thus, the enhancement of thermal and electrical performance of PVT systems can be achieved by implying jet impingement cooling mechanism.

Based on the literature, there is insufficient study on the cooling of bifacial PVT systems with jet air impingement. Therefore, this work aims to evaluate the exergetic performance of a jet impingement bifacial PVT (JIBPVT) solar air collector with different packing factors and jet distributions. A novel dual-functional jet plate reflector was developed to assist the light reflection onto the rear part of the bifacial PV panel while simultaneously introducing an impinging air jet for cooling. The exergetic analysis was conducted through an indoor experiment. The effects of air mass flow rate, solar irradiance, packing factors of bifacial PV modules and the jet plate reflectors with different geometric configurations on the exergetic performance were examined and discussed.

Experimental setup

Description of JIBPVT

The schematic cross-sectional image of the bifacial PVT and the direction of airflow and light transmission are illustrated in Figure and Figure , respectively. A bifacial PV panel, a jet plate reflector, and an insulated backplate formed the collector. Additionally, this system contains of two channels: one between the bifacial PV panel and the jet plate reflector, and another between the jet plate reflector and the backplate. Air from the surrounding region entered the lower channel first before passing through the perforations in the jet plate reflector and entering the upper channel. Then, the air entered the top channel at a high rate of speed and impacted the bifacial solar panel's bottom part. This is where heat transmission between the bifacial solar panel and the ambient air occurred. The suggested design has a length of 0.7 m, a width of 0.68 m, and a height of 0.12 m, which is according to the dimensions of the bifacial solar panels. Each airflow channel was set at a length of 0.025 m. The experiment was conducted on a bifacial solar panel with packing factors of 0.22, 0.33, and 0.66 with air mass flow rates in the range between 0.014 and 0.035 kg/s. The variable and fixed design and operational parameters are shown in Table 1 [17].

Design of holes on jet plate reflector

This study suggested using a jet plate reflector on the backside of the bifacial solar panel to increase cooling and light absorption. The holes of jet plate reflectors were sized and arranged to match the PV cells' dimensions and configuration in a real-world bifacial PV panel. Three separate jet plate reflectors are illustrated in Figure to Figure , each having a unique streamwise pitch of X=0.09 m, 0.105 m, and 0.126 m; a unique spanwise pitch of Y=0.081 m, 0.0945 m, and 0.1134 m; and a unique variety of holes N=64, 49, and 36. The jet plate reflector's thickness was set to 0.001 m, while the diameter of each jet hole, D_j was set to 0.003 m.

Assumptions for exergy analysis

The assumptions are made for exergy analysis [7], [12]:

i. The thermal configurations of the PV cells, laminate, jet plate reflector and components of solar collector are neglected.

ii. The sum of front and rear electricity generations of the PV module is the overall electricity generation of the module.

iii. The front and rear sides of bifacial PV module are assumed to have the similar temperature.

iv. The heat transfer inside the collector is caused by forced convection.

v. The only temperature gradient is only along the length of the collector.

vi. Uniform air flow distribution inside the channel occurs along the collector's width.

vii. The heat transfer flow is exclusively perpendicular to the cross section of the channel.

viii. Thermal losses at the SAC edges are negligible.

ix. There are no leaks in the airflow paths.

x. The physical characteristics of air are considered to remain constant as insignificant temperature variation.

xi. Within the encapsulation glasses, the PV cells are in perfect thermal contact, and both have the same uniform temperature across the panel.

Exergy efficiency, exergy destruction, improvement potential

For the improvement potential, IP can be calculated by [18]:

$$IP = (1 - nx)Exd \tag{1}$$

where the exergy efficiency, nx can be calculated by [19]:

$$nx = \frac{Ex_{output}}{Ex_{input}} \tag{2}$$

where the total exergy output, Ex_{output} can be calculated by:

$$Ex_{output} = Ex_{thermal} + Ex_{electrical} \tag{3}$$

where the thermal exergy of the system, $Ex_{thermal}$ can be calculated by:

$$Ex_{thermal} = Qu \times (1 - (\frac{T_a}{T_{out}})) \tag{4}$$

where useful heat gain, Qu can be calculated by [20]:

$$Q_u = \dot{m}C_p(T_{out} - T_i) \quad (5)$$

The electrical exergy of the system, $Ex_{electrical}$ can be identified by:

$$Ex_{electrical} = P_{max}(1 - \left(\frac{4}{3}\right)\left(\left(\frac{T_a}{T_{sun}}\right) + \left(\frac{1}{3}\right)\left(\frac{T_a}{T_{sun}}\right)^4\right)) \quad (6)$$

where electrical power generated, P_{max} can be identified by [21]:

$$P_{max} = IA_c\alpha_{pv}P\left(n_{pv,front}\right) + IA_c\tau_l(1-P)n_R\alpha_{pv}P(n_{pv,rear}) \quad (7)$$

where front & rear part of bifacial PV cell efficiency, $n_{pv,front}$ & $n_{pv,rear}$ can be calculated by [12]:

$$n_{pv,front} = n_{pv,rear} = n_{ref}(1 - B(T_{pv} - T_{ref}) \quad (8)$$

For the total exergy input, Ex_{input} can be identified by [22]:

$$Ex_{input} = \mathrm{A_c} \times \mathrm{I} \times (1 - (\frac{4}{3})((\frac{T_a}{T_{sun}}) + (\frac{1}{3})(\frac{T_a}{T_{sun}})^4)) \quad (9)$$

For the exergy destruction, Exd can be calculated by [23]:

$$Exd = T_a s_{gen} \quad (10)$$

where the entropy generation rate, s_{gen} can be calculated by:

$$s_{gen} = ((\frac{1}{T_a} - \frac{1}{T_{sun}})Qs) + (\ln(\frac{T_{out}}{T_i}) - (\frac{T_{out}}{T_a}) + (\frac{T_i}{T_a}))\dot{m}C_p \quad (11)$$

where the total solar energy absorbed, Qs can be calculated by:

$$Qs = (I\alpha_{pv}P + I\alpha_l(1-P) + I\tau_l(1-P)n_R\alpha_{pv}P + I\tau_l(1-P)n_R\alpha_l(1 - P) + I\tau_l(1-P)(1-n_R))Ac \quad (12)$$

For hydraulic diameter, D_h is given by:

$$D_h = (\frac{4Wd}{2(W+d)}) \quad (13)$$

For Reynolds number, Re is given by:

$$Re = \frac{\dot{m} D_h}{W d \mu} \quad (14)$$

Experimental Procedure

An experiment was done to determine the exergy performance of JIBPVT. The indoor experiment setup with necessary instrumentation for JIBPVT is depicted in

Figure . The prototype includes a bifacial PV panel, collector body, and jet plate reflector based on the concept described before in Table 1. Solar simulators with six rows of a total of 48 halogen lights were positioned at the top of the testing section to generate a heat flux to approximate the solar irradiance. Each lamp measures 118 mm in length and delivers 500 W of heat flux. Similar heat flux intensity was used in the study [12] with similar dimensions of bifacial PV panels. The intensity of heat flux was regulated by digital voltage controllers and monitored by utilizing a pyranometer. In addition, the entry and exit of the collector were linked to an insulated black box or manifolds to avoid heat loss to the environment. The temperature readings were acquired from several places around the collector by utilizing standardized 0.2 mm of K-Type thermocouples linked to a data acquisition. At the same time, the inlet and exit air wind speeds were monitored by utilizing an anemometer. Although the emphasis of the study was forced convection mode, it is essential to utilize a blower or fan that can manage the collector's required volume of air and heat. Finally, a DC electronic load was utilized to measure the I-V curve of the PV panel.

The experimental observations have been done following [18], [23]. Fourteen thermocouples will first be placed around the collector. Then, by changing the voltage controller, the blower's velocity and the solar simulator's solar irradiance were established. For each experiment set, temperature readings from thermocouples surrounding the collector were gathered for 30 minutes using a data recorder (at 30-second intervals). Before capturing data, the data logger aided in establishing a steady condition. Before data collection, a stable condition was established. Stable conditions were most likely attained when no substantial temperature changes were noted for 20 minutes between consecutive examinations. The I-V curve was displayed using the electronic load during the final ten minutes of the experiment. After data collection was completed, the collector was cooled for two hours before commencing the following experiments with a new manipulating parameter and operational conditions. Following that, the data was analyzed using the equations from (1) to **Error! Reference source not found.**). Consequently, the following parameters were recorded for each of the experiment's scanning cycles: (a) The bifacial PV panel's average temperature, T_p; (b) The average temperature of the air entering the system, the air leaving the system, and the ambient air, T_i, T_o, T_a; (c) The solar irradiance, I; (d) The mass flow rate, $\dot{m}$; (e) The I-V curve.

Uncertainty analysis

Uncertainty analysis is often used terms to refer to the process of analyzing the uncertainty associated with a measurement result. A comprehensive description of a measured value should include an estimation of the value's confidence level. Errors and uncertainties can occur due to instrument selection, condition, calibration, environment, observation, reading, and test design.

For instance, the current experiment evaluated temperatures, solar irradiance, and mass flow rate using suitable sensors. The uncertainty associated with parameter measurements is shown in Table 2, which is referring to the calculation in [24].

The mass flow rate, $\dot{m}$ is obtained by:

$$\dot{m} = \rho V A \tag{15}$$

where ρ= air density, V=outlet air velocity, A=cross-sectional area of the pipe. Hence, $\dot{m} = f(\rho, V, A)$ where the fractional uncertainty for mass flow rate, $\frac{\omega \dot{m}}{\dot{m}}$ is:

$$\frac{\omega \dot{m}}{\dot{m}} = \left[\left(\frac{\omega_T}{T}\right)^2 + \left(\frac{\omega_v}{v}\right)^2 + 4\left(\frac{\omega_r}{r}\right)^2\right]^{1/2} \tag{16}$$

where $\frac{\omega_T}{T}$, $\frac{\omega_v}{v}$, $\frac{\omega_r}{r}$ are the fractional uncertainty for ambient air temperature, outlet air velocity and radius of pipe, which are 0.0016, 0.0021, 0.005, respectively. The fractional uncertainties for solar intensity and temperature difference, $\frac{\omega_I}{I}$ and $\frac{\omega_{\Delta T}}{\Delta T}$ are 0.035 and 6.55 × 10^{-6}, respectively.

The calculations show that percent uncertainty in the mass flow rate is 1.03%.

Results and Discussions

Exergy efficiency may be a more critical metric than energy efficiency because it provides a more detailed picture of performance. The exergy efficiency demonstrates the importance of assessing losses and internal irreversibility to optimize the performance of a SAC. The relationship between exergy efficiency and different design and operational parameters is investigated using graphical representations.

Thermal exergy

The effect of mass flow rate on thermal exergy of JIBPVT with different jet plate reflectors and packing factors are demonstrated graphically in Figure and Figure , respectively. The results obtained by JIBVPT with 36-holes jet plate reflectors and 0.66 packing factor are slightly higher than other designs. Under solar irradiance of 900 W/m^2 and mass flow rate of 0.014-0.035 kg/s, the thermal exergy of JIBPVT with 36, 49 and 64 holes are 5.60-7.92 W, 5.50-7.69 W, and 5.40-7.49 W, respectively. This is due to 36-holes jet plate reflector has larger spanwise and streamwise pitches, which led to lesser crossflow effect and jet interference. Hence, more heat transfer occurred between the air flow and the bottom part of the bifacial PV panel. Therefore, JIBPVT with 36 holes has the optimum thermal exergy. Under similar operating parameters, the thermal exergy of JIBPVT with packing factors of 0.22, 0.33 and 0.66 are 3.57-5.45 W, 4.21-6.28 W, and 5.60-7.92 W, respectively. Higher thermal gain can be observed from the bifacial PV panel with 0.66 packing factor due to larger area of light absorption. Hence, more heat was absorbed. Therefore, higher packing factor of JIBPVT will have a higher thermal exergy. Similar trend of results were observed by the investigation reported by Chauhan et. al [25].

Electrical exergy

The influence of mass flow rate on the electrical exergy of JIBPVT with various jet plate reflectors and packing factors is graphically depicted in Figure and

Figure 0, respectively. JIBVPT's findings with 36-hole jet plate reflectors and a packing factor of 0.66 are marginally better than those obtained with other designs. The electrical exergy of JIBPVT with 36, 49, and 64 holes is 39.70-42.21 W, 39.55-42.08 W, 39.42-41.97 W, respectively, when solar irradiance is 900 W/m^2 and mass flow rate is 0.014-0.035 kg/s. As mentioned in the last sub-section for the thermal exergy, higher heat transfer rate was observed in JIBPVT with 36-holes. The bifacial PV module operated in lower temperature and produced higher electricity, which contributed to higher electrical exergy. The electrical exergy of JIBPVT with packing factors of 0.22, 0.33, and 0.66 is 17.13-17.76 W, 24.10-24.17 W, 39.70-42.21 W, respectively, under equivalent working conditions. Higher electricity generation was observed in JIBPVT with 0.66 packing factor due to larger area of light absorption and higher electricity generation. [12] reported similar observations in their experiments.

Overall exergy

The effects of solar irradiance on thermal and electrical exergies are shown in

Figure and

Figure , respectively. Highest thermal exergy of 7.92 W is observed at the highest solar irradiance of 900 W/m^2 while lowest thermal exergy of 0.62 W is observed at the lowest solar irradiance of 300 W/m^2. For electrical exergy, the highest and lowest values are 42.2 W and 14.7

W, which can be found at highest and lowest solar irradiance of 900W/m^2 and 300 W/m^2, respectively. Increased solar irradiance increases the collector's and bifacial PV module heat gain, which led to higher temperature within collector and PV temperature. Thus, thermal exergy will increase, and the PV module will operate at a higher temperature, which led to a reduce in its electrical exergy output. However, increased solar irradiance increases the PV module electricity generation, raising the electrical exergy output. Therefore, due to solar irradiance being the primary significant factor to electrical exergy output, reducing electrical exergy due to the temperature of PV module increases has been overcome. These observations were also supported by earlier reported study [12].

The variations of exergy efficiency versus Reynolds number and solar irradiance are illustrated in Figure . The exergy efficiency of the system improves up to a Re of 3537, which is within the transition flow region, then begins to fall owing to higher exergy destruction. From Figure , it is confirmed that the improvement potential and exergy destruction correspondingly increase as the Reynolds number increases. The optimum operating Reynolds number for this system is 3537 or mass flow rate of 0.025 kg/s to produce maximum exergy efficiency. The highest exergy efficiency of JIBPVT is 11.88 %, with bifacial PV module of 0.66 packing factor and jet plate reflector with 36-holes, at 900 W/m^2 solar irradiances and a Re of 3537. Moreover, higher solar irradiance improved the exergy efficiency of the system by increasing the thermal and electrical exergy gain. From the figure, the highest exergy efficiency can be observed at the highest solar irradiance. In general, exergy efficiency is directly proportional to solar irradiance. A similar pattern of results was observed in the study of [18].

The exergy of the system is plotted against the solar irradiance in Figure . The highest total exergy output of JIBPVT is 47.87 W when bifacial PV module with 0.66 packing factor are used in conjunction with a 36-hole jet plate reflector, solar irradiance of 900 W/m^2, and a Re of 3537. Thus, it can be demonstrated that JIBPVT's electrical exergy contributes the most to its total exergy output. The total exergy input is directly proportional to the total solar irradiance input at the surface of the collector. The highest total exergy input for this investigation is 402.8 W. In the second law of thermodynamics, the total exergy destruction, also known as the dissipated power for irreversible process, can be calculated from the entropy generation rate and ambient temperature. The highest dissipated power went up to 345 W/m^2 at highest solar irradiance. While the exergy destruction of the irreversible process is minimized, the exergy efficiency improvement is maximized. Therefore, the concept of exergetic "Improvement Potential" (IP) may be a handy tool for analyzing systems or processes more efficiently. From the results, it can be observed that the highest IP achieved 304 W. Overall, the input, output, destruction exergies and improvement potential of the proposed system is directly proportional to the solar irradiance. This pattern of observation has been shown in previous works [22].

Data comparison

The overall exergy efficiency observed in the present work are compared with earlier reported studies in

Table 0. Among all the air based solar system compared, the present study has achieved the highest exergy efficiency of 11.88 %. By comparing findings from previous research that employed a comparable bifacial PV panel [12], the efficiency of total exergy has been increased by 3.48 %.

Recommendations for future work

The current study goal is to evaluate experimentally and numerically the influence of jet air impingement on the thermal and electrical performance of a solar thermal collector. However, there are many critical heat transfer enhancement characteristics of jet impingement in solar thermal collectors that need to be studied, and a few recommendations for additional research were made:

- Different types of bifacial PV cells such as poly-crystalline silicon and thin film can be used as only mono-crystalline silicon PV cell was used in this research. It is ideal to find the best type of bifacial PV cells for optimum performance.
- External reflector or Fresnel lens can be used to reflect or concentrate the solar radiation at the front side of the bifacial PV module. However, the increment of the PV temperature must be noticed to prevent the PV module operates at high temperature, which led to lower electrical efficiency.

- Phase change materials (PCM) could be used as an effective method of storing thermal energy from solar. The PCM could be attached at the rear part of the solar collector, below the backplate.

Conclusion

The exergetic performance of JIBPVT solar air collector with different packing factors and jet distributions was evaluated experimentally. On the performance of the JIBPVT, the impacts of mass flow rate, solar irradiation, types of jet plate reflector, and packing factor of the bifacial PV module were examined and discussed. The following are the key findings of this research:

- Bifacial PVT modules with a higher solar irradiance and packing factor provide higher thermal and electrical exergies.
- The 36-hole jet plate reflector has a wider spacing between jet holes, which reduces jet interference and the crossflow effect, resulting in a faster heat transfer rate.
- Increased mass flow rate reduces the thermal exergy but increase electrical exergy output of the system.
- Under 0.66 packing factor of bifacial PVT module with 36-holes jet plate reflector, the maximum thermal, electrical and total exergy output of JIBPVT are 7.9 W, 42.2 W, and 53.4 W, respectively.
- The highest exergy input, exergy destruction and improvement potential of the proposed system are 403 W, 346 W and 305 W, respectively.

- The input, output, destruction exergies and improvement potential of the proposed system is directly proportional to the solar irradiance.
- A comparison of JIBPVT's total exergy efficiency with that of earlier research was also made. The JIBPVT outperformed other air-based PVT systems, with an exergy efficiency of 11.88%. As a result, the proposed system is a very efficient solar collector.

Nomenclature

A	cross-sectional area of the pipe
A_c	the total surface area of the collector (m^2)
B	temperature coefficient
C_p	specific heat of the air (J/(kg. K))
CPC	compound parabolic collector
d	duct depth for each channel
D_h	the hydraulic diameter of the air channel (m)
D_j	the diameter of jet holes (m)
$Ex_{electrical}$	electrical exergy
Exd	exergy destruction
Ex_{input}	total exergy input
Ex_{output}	total exergy output
$Ex_{thermal}$	thermal exergy
I	solar irradiance (W/m^2)
IP	improvement potential
JIBPVT	jet impingement bifacial PVT
$\dot{m}$	air mass flow (kg/s)
n	efficiency
nx	exergy efficiency
P	packing factor of PV cell
P_{max}	electrical power generated

PV	photovoltaic
PVT	photovoltaic-thermal
Qs	total solar energy absorbed
Q_u	useful heat gain (W)
r	radius of pipe
Re	Reynolds number
s_{gen}	entropy generation rate
SAC	solar air collector
Si-C	silicon carbide
T	temperature (K)
V	outlet air velocity
W	width of collector
X	streamwise pitch (m)
Y	spanwise pitch (m)

Greek Symbols

μ	air viscosity (kg/ms)
α	absorptivity
ρ	air density (kg/m^3)
τ	transmissivity
ω	uncertainty

Subscripts

a	ambient air
c	collector
i	inlet air
j	jet hole
l	lamination
out	outlet air
p	bifacial photovoltaic panel's average temperature
pv	bifacial pv cell
R	reflectivity of jet plate reflector
ref	reference condition
sun	the sun

Acknowledgments

The authors would like to thank UKM for its funding (GUP-2018-128).

References

[1] C. Choudhury and H. P. Garg, "Evaluation of a jet plate solar air heater," *Sol. Energy*, vol. 46, no. 4, pp. 199–209, 1991, doi: 10.1016/0038-092X(91)90064-4.

[2] M. Belusko, W. Saman, and F. Bruno, "Performance of jet impingement in unglazed air collectors," *Sol. Energy*, vol. 82, no. 5, pp. 389–398, 2008, doi: 10.1016/j.solener.2007.10.005.

[3] R. Chauhan and N. S. Thakur, "Heat transfer and friction factor correlations for impinging jet solar air heater," *Exp. Therm. Fluid Sci.*, vol. 44, pp. 760–767, 2013, doi: 10.1016/j.expthermflusci.2012.09.019.

[4] R. Chauhan and N. S. Thakur, "Investigation of the thermohydraulic performance of impinging jet solar air heater," *Energy*, vol. 68, pp. 255–261, 2014, doi: 10.1016/j.energy.2014.02.059.

[5] R. Chauhan, T. Singh, N. S. Thakur, and A. Patnaik, "Optimization of parameters in solar thermal collector provided with impinging air jets based upon preference selection index method," *Renew. Energy*, vol. 99, pp. 118–126, 2016, doi: 10.1016/j.renene.2016.06.046.

[6] H. Y. Chan, A. A. Vinson, S. S. S. Baljit, and M. H. Ruslan, "Comparison of Thermal Performances between Low Porosity Perforate Plate and Flat Plate Solar Air Collector," *J. Phys. Conf. Ser.*, vol. 989, no. 1, 2018, doi: 10.1088/1742-6596/989/1/012001.

[7] M. M. Matheswaran, T. V. Arjunan, and D. Somasundaram, "Analytical investigation of solar air heater with jet impingement using energy and exergy analysis," *Sol. Energy*, vol. 161, no. October 2017, pp. 25–37, 2018, doi: 10.1016/j.solener.2017.12.036.

[8] W. E. Ewe, A. Fudholi, K. Sopian, N. Asim, Y. Ahmudiarto, and A. Salim, "Overview on

Recent PVT Systems with Jet Impingement," *Int. J. Heat Technol.*, vol. 39, no. 6, pp. 1951–1956, 2021, doi: 10.18280/ijht.390633.

[9] M. Jaszczur, J. Teneta, Q. Hassan, E. Majewska, and R. Hanus, "An Experimental and Numerical Investigation of Photovoltaic Module Temperature Under Varying Environmental Conditions," *Heat Transf. Eng.*, vol. 42, no. 3–4, pp. 354–367, 2021, doi: 10.1080/01457632.2019.1699306.

[10] M. Chaabane, H. Mhiri, and P. Bournot, "Performance optimization of water-cooled concentrated photovoltaic system," *Heat Transf. Eng.*, vol. 37, no. 1, pp. 76–81, 2016, doi: 10.1080/01457632.2015.1042344.

[11] S. A. Brideau and M. R. Collins, "Development and validation of a hybrid PV/Thermal air based collector model with impinging jets," *Sol. Energy*, vol. 102, pp. 234–246, 2014, doi: 10.1016/j.solener.2014.01.022.

[12] P. Ooshaksaraei, K. Sopian, S. H. Zaidi, and R. Zulkifli, "Performance of four air-based photovoltaic thermal collectors configurations with bifacial solar cells," *Renew. Energy*, vol. 102, pp. 279–293, 2017, doi: 10.1016/j.renene.2016.10.043.

[13] H. A. Hasan, K. Sopian, A. H. Jaaz, and A. N. Al-Shamani, "Experimental investigation of jet array nanofluids impingement in photovoltaic/thermal collector," *Sol. Energy*, vol. 144, pp. 321–334, 2017, doi: 10.1016/j.solener.2017.01.036.

[14] H. A. Hasan, K. Sopian, and A. Fudholi, "Photovoltaic thermal solar water collector designed with a jet collision system," *Energy*, vol. 161, pp. 412–424, 2018, doi: 10.1016/j.energy.2018.07.141.

[15] A. H. Jaaz, K. Sopian, and T. S. Gaaz, "Study of the electrical and thermal performances

of photovoltaic thermal collector-compound parabolic concentrated," *Results Phys.*, vol. 9, pp. 500–510, 2018, doi: 10.1016/j.rinp.2018.03.004.

[16] M. Javidan and A. J. Moghadam, "Experimental investigation on thermal management of a photovoltaic module using water-jet impingement cooling," *Energy Convers. Manag.*, vol. 228, no. November 2020, p. 113686, 2021, doi: 10.1016/j.enconman.2020.113686.

[17] W. E. Ewe, A. Fudholi, K. Sopian, and N. Asim, "Modeling of bifacial photovoltaic-thermal (PVT) air heater with jet plate," *Int. J. Heat Technol.*, vol. 39, no. 4, pp. 1117–1122, 2021, doi: 10.18280/ijht.390409.

[18] A. Fudholi, K. Sopian, M. Y. Othman, M. H. Ruslan, and B. Bakhtyar, "Energy analysis and improvement potential of finned double-pass solar collector," *Energy Convers. Manag.*, vol. 75, pp. 234–240, 2013, doi: 10.1016/j.enconman.2013.06.021.

[19] A. Lingayat, V. P. Chandramohan, and V. R. K. Raju, "Energy and Exergy Analysis on Drying of Banana Using Indirect Type Natural Convection Solar Dryer," *Heat Transf. Eng.*, vol. 41, no. 6–7, pp. 551–561, 2020, doi: 10.1080/01457632.2018.1546804.

[20] S. Singh and P. Dhiman, "Thermal and thermohydraulic efficiency of recyclic-type double-pass solar air heaters with fins and baffles," *Heat Transf. Eng.*, vol. 37, no. 15, pp. 1302–1317, 2016, doi: 10.1080/01457632.2015.1119619.

[21] X. Sun, M. R. Khan, C. Deline, and M. A. Alam, "Optimization and performance of bifacial solar modules: A global perspective," *Appl. Energy*, vol. 212, no. 1, pp. 1601–1610, 2018, doi: 10.1016/j.apenergy.2017.12.041.

[22] A. Ibrahim, A. Fudholi, K. Sopian, M. Y. Othman, and M. H. Ruslan, "Efficiencies and improvement potential of building integrated photovoltaic thermal (BIPVT) system,"

Energy Convers. Manag., vol. 77, pp. 527–534, 2014, doi: 10.1016/j.enconman.2013.10.033.

[23] A. Fudholi, K. Sopian, M. H. Ruslan, and M. Y. Othman, "Performance and cost benefits analysis of double-pass solar collector with and without fins," *Energy Convers. Manag.*, vol. 76, pp. 8–19, 2013, doi: 10.1016/j.enconman.2013.07.015.

[24] R. Vaziri, M. Ilkan, and F. Egelioglu, "Experimental performance of perforated glazed solar air heaters and unglazed transpired solar air heater," *Sol. Energy*, vol. 119, pp. 251–260, 2015, doi: 10.1016/j.solener.2015.06.043.

[25] R. Chauhan, N. S. Thakur, T. Singh, and M. Sethi, "Exergy based modeling and optimization of solar thermal collector provided with impinging air jets," *J. King Saud Univ. - Eng. Sci.*, vol. 30, no. 4, pp. 355–362, 2018, doi: 10.1016/j.jksues.2016.07.003.

[26] R. Saidur, G. Boroumandjazi, S. Mekhlif, and M. Jameel, "Exergy analysis of solar energy applications," *Renew. Sustain. Energy Rev.*, vol. 16, no. 1, pp. 350–356, 2012, doi: 10.1016/j.rser.2011.07.162.

Table 1 Variable and fixed design & operating parameters

Parameters	Base values
Variable design & operating parameters	
Air mass flow rate, $\dot{m}$	0.014 - 0.035 kg/s
No of PV cells	4, 6, 12
Number of jet holes, N	64, 49, 36
Packing factor, P	0.22, 0.33, 0.66
Solar irradiance, I	300 - 900 W/m^2
Spanwise pitch, Y	0.081, 0.0945, 0.01134
Streamwise pitch, X	0.09, 0.105, 0.126
Fixed design & operating parameters	
Absorptivity of lamination, α_l	0.1
Absorptivity of PV cell, α_{pv}	0.91
Diameter of jet holes, D_j	0.003 m
Duct depth for each channel, d	0.025 m
Electrical efficiency at a reference condition, n_{ref}	0.16
Temperature coefficient, B	0.0045 K^{-1}
The reflectivity of jet plate reflector, n_R	0.7
The temperature at a reference condition, T_{ref}	298 K
The temperature of the sun, T_{sun}	5778 K
The thickness of the jet plate reflector	0.001 m
The transmittance of lamination, τ_l	0.85

Width of collector, W	0.684 m

Table 0 Relative uncertainty during measurements of the parameters.

Parameters	Fractional Uncertainty
Ambient air temperature	0.0016
Outlet air velocity	0.0021
Radius of pipe	0.005
Solar intensity	0.035
Temperature difference	6.55×10^{-6}
Mass flow rate of air	1.03%

Table 0 Comparison of prior research' exergy efficiency

Types of solar collector	n_{exergy} (%)	References
Bifacial PVT SAC with jet plate reflector	11.88	Present Study
The unglazed air-based PVT system	10.75	[26]
The (glass-to-glass) air-based PVT system	10.45	[26]
Bifacial PVT air collector with semi-mirror reflector	8.40	[12]
Double-pass jet impingement SAC with arc roughness absorber plate	4.36	[7]
Unglazed air-based PVT system integrated greenhouse	4.00	[26]

List of Figure Captions

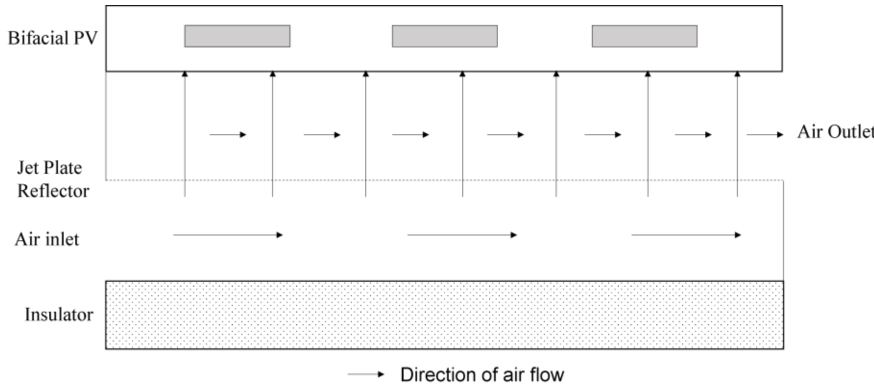

Figure 1 The direction of airflow of JIBPVT

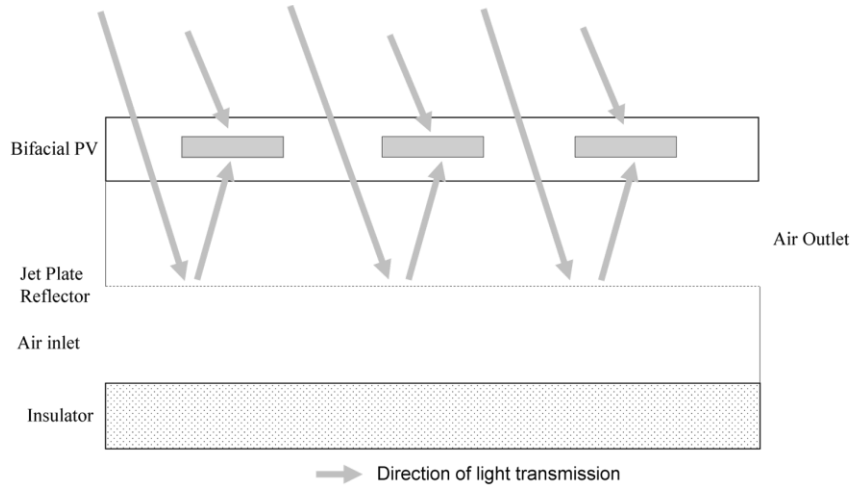

Figure 2 The direction of light transmission of JIBPVT

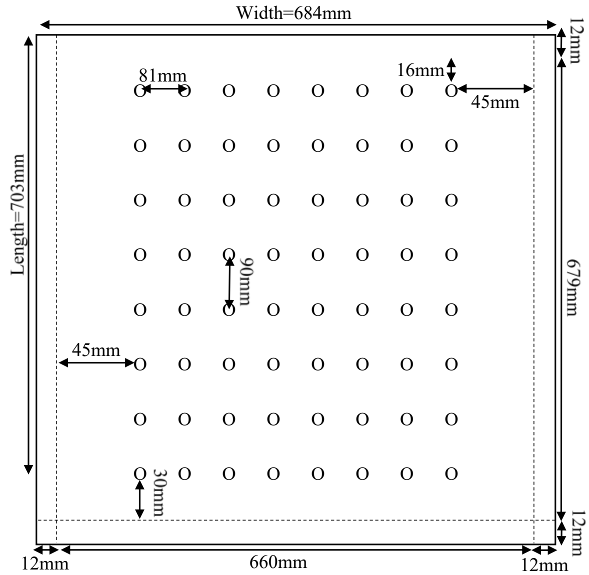

Figure 3 Jet plate with 64 holes, X=0.09 m & Y=0.081 m

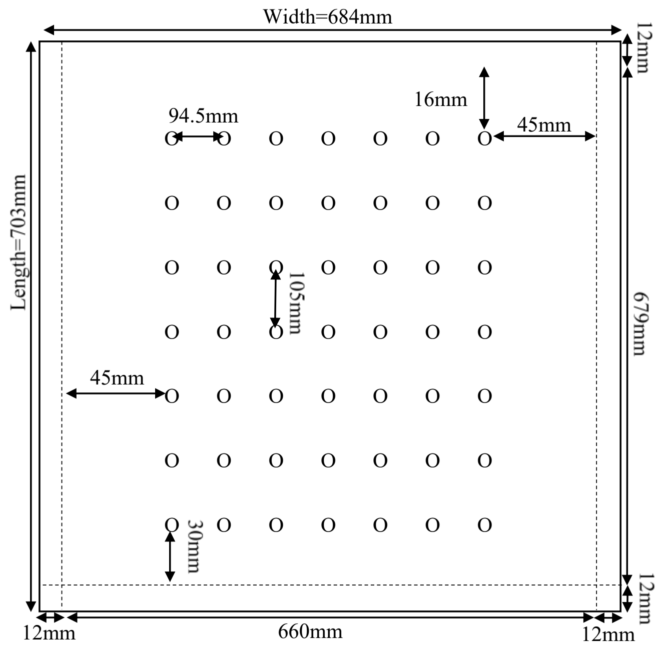

Figure 4 Jet plate with 49 holes, X=0.105 m & Y=0.0945 m

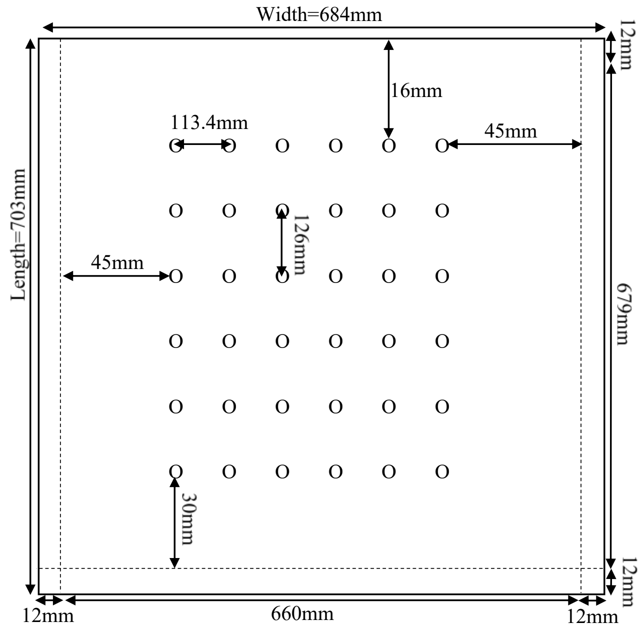

Figure 5 Jet plate with 36 holes, X=0.126 m & Y=0.1134 m

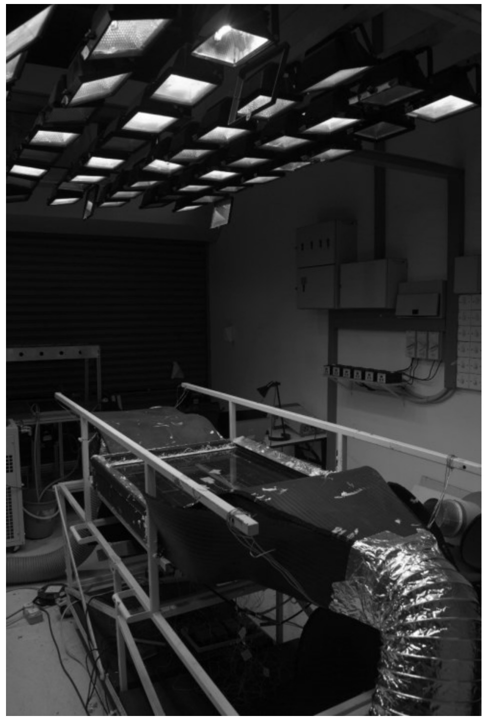

Figure 6 Indoor experiment setup for JIBPVT

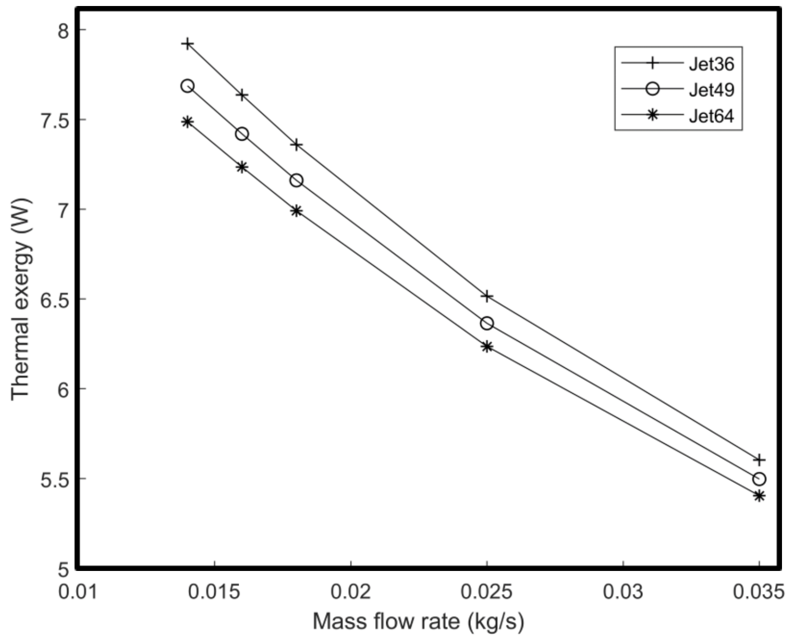

Figure 7 Effect of mass flow rate on thermal exergy of JIBPVT with different jet plate reflectors

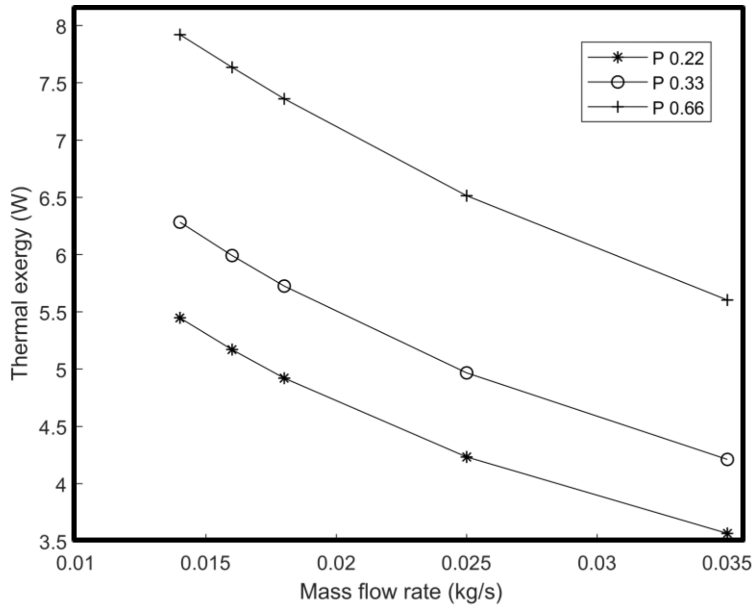

Figure 8 Effect of mass flow rate on thermal exergy of JIBPVT with different packing factors

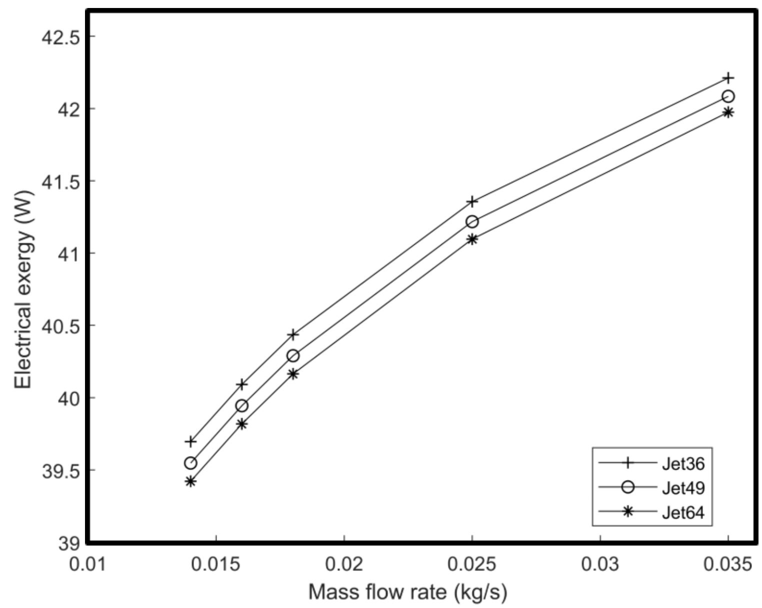

Figure 9 Effect of mass flow rate on electrical exergy of JIBPVT with different jet plate reflectors

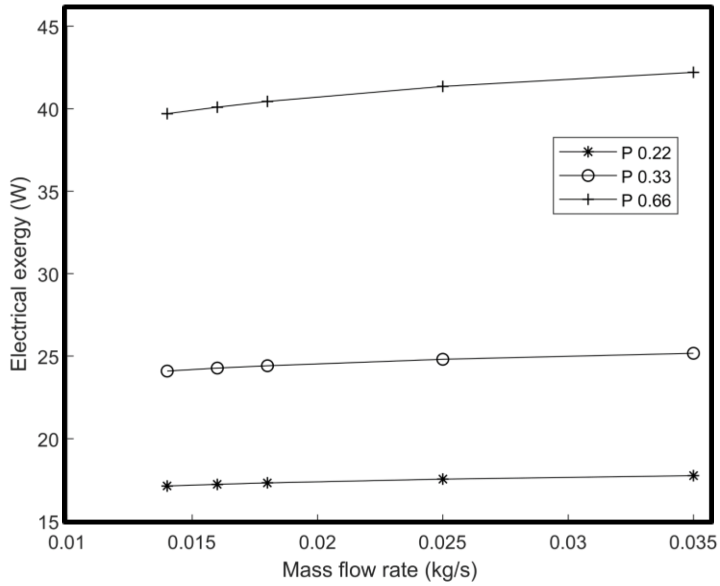

Figure 10 Effect of mass flow rate on electrical exergy of JIBVPT with different packing factors

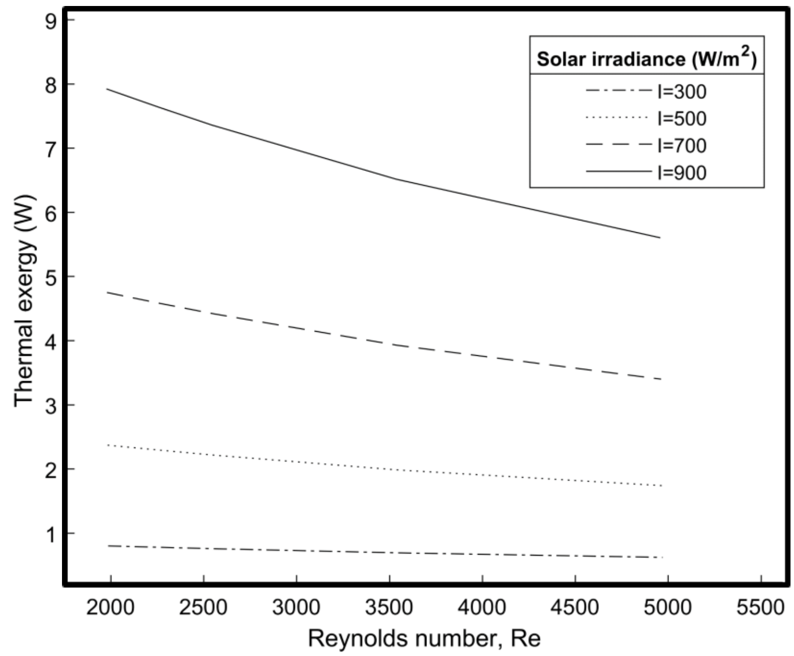

Figure 11 Effect of solar irradiance on thermal exergy of JIBPVT

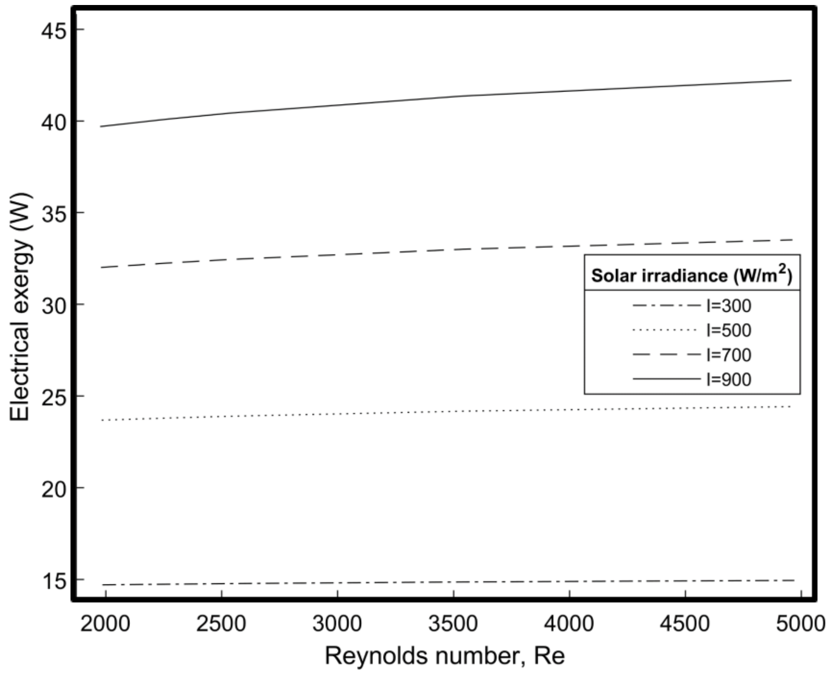

Figure 12 Effect of solar irradiance on electrical exergy of JIBPVT

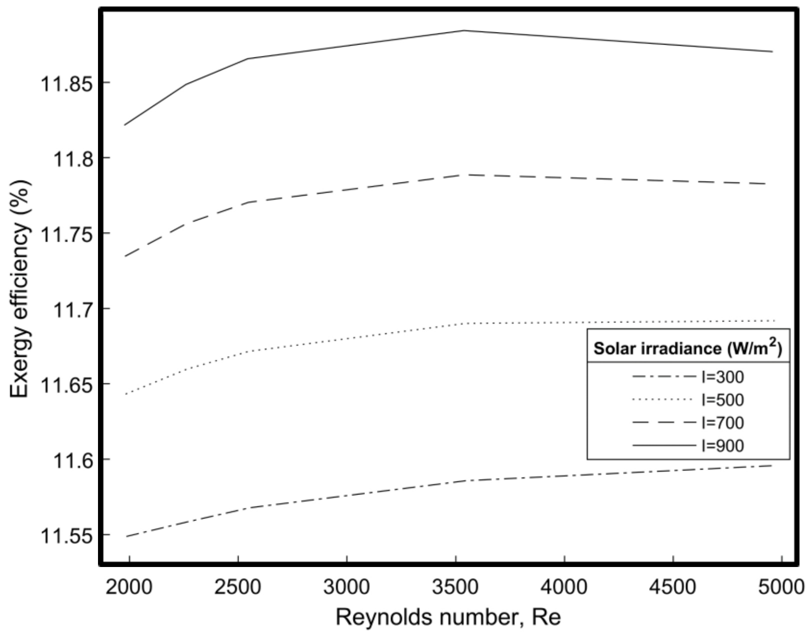

Figure 13 Effects of solar irradiance and Re on exergy efficiency of JIBPVT

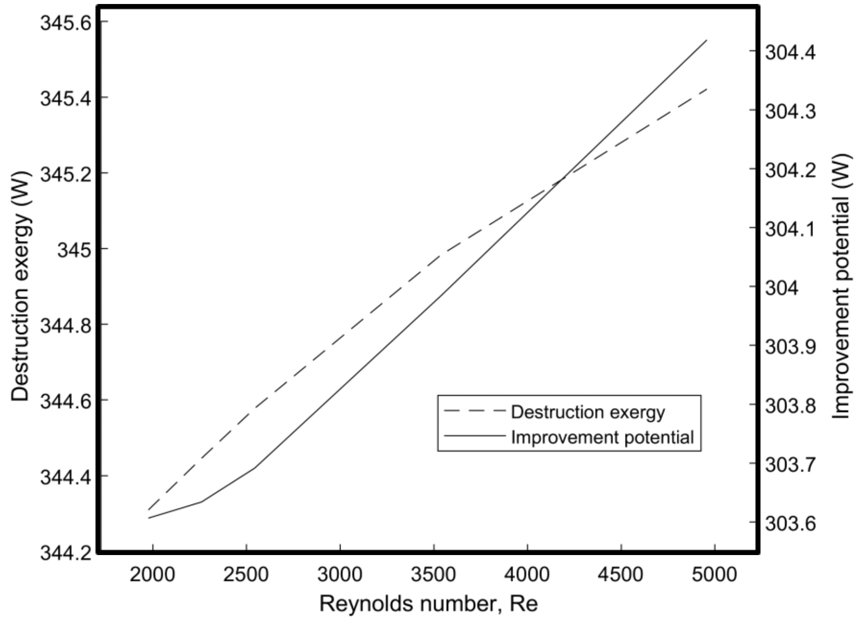

Figure 14 Effects of Re on destruction exergy and IP of JIBPVT

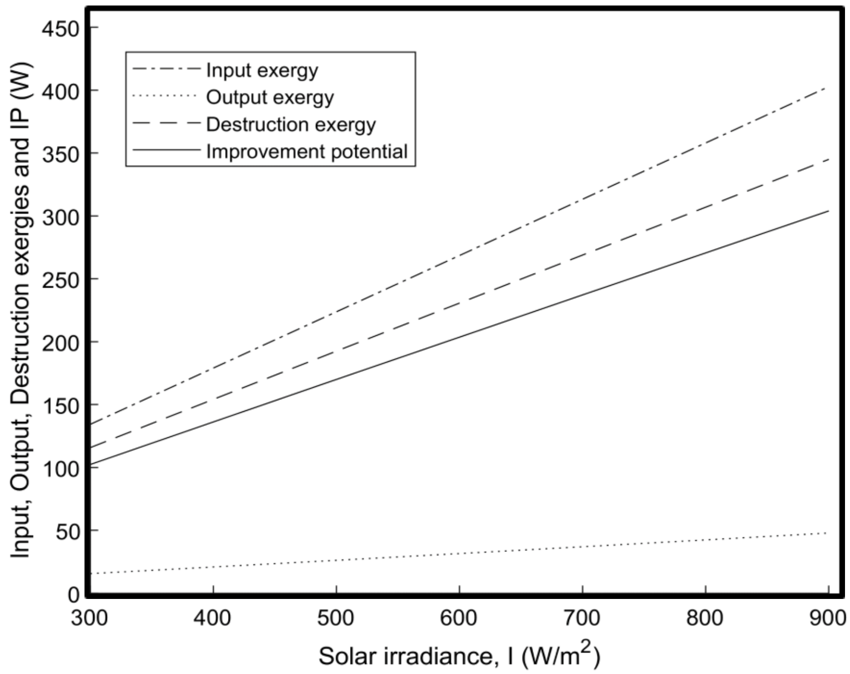

Figure 15 Effects of solar irradiance on input, output, destruction exergies and improvement potential

Notes on contributors

Win Eng Ewe is a Ph.D. student at Solar Energy Research Institute (SERI), Universiti Kebangsaan Malaysia (UKM), Bangi, Malaysia. He received the M.Sc. degree in Energy Technology from UKM and B.S.c. degree in Physics from University of Glasgow, United Kingdom. He is currently preparing his thesis and working on Bifacial Photovoltaic-Thermal (PVT) Solar Air Collector With Jet Impingement.

Kamaruzzaman Sopian graduated with the BS Mechanical Engineering from the University of Wisconsin-Madison in 1985, the MS in Energy Resources University of Pittsburgh in 1989 and PhD in Mechanical Engineering from the Dorgan Solar Laboratory, University of Miami-Coral Gables. His main contributions are in solar radiation modeling and resource assessment, advanced solar photovoltaic systems (grid-connected photovoltaic, solar powered regenerative fuel cell, solar hydrogen production, thin film silicon solar cell) and advanced solar thermal systems (solar cooling, solar heat pump, solar assisted drying, combined photovoltaic thermal or hybrid collector). A Fellow of the Malaysia Academy of Sciences and listed in the 2019- 2021 Highly Cited Researchers by the Web of Science

Group, Clarivate Analytics.

Dr. M. Mohanraj has completed his Bachelor degree in Mechanical Engineering from University of Madras during the year 1999, Master's degree in Refrigeration and Air Conditioning from Bharathiar University during the year 2001 and Ph.D degree from National Institute of Technology, Calicut during the year 2009. Presently, he is associated with Hindusthan College of Engineering and Technology, Coimbatore. He has wide experience in developing heat pump systems for drying, water heating, space heating and desalination applications. He has published more than 90 technical papers in leading international journals in the field of heat pumps, renewable energy applications, materials etc. He has been associated with Al FarabiKazah National University as collaborative research work on heat pumps for space heating applications.

Ahmad Fudholi, Ph.D, joined the SERI as a lecturer in 2014. He involved more than USD 500,000 worth of research grant (24 grant/project). He supervised and completed more than 30 M.Sc and Ph.D students. His current research focus is renewable energy, particularly solar energy technology, micropower systems, solar drying systems and advanced solar thermal systems (solar-assisted drying, solar heat pumps, PV/T systems). He has published more than 300 peer-reviewed papers, of which 65 papers are in the WoS index (50 Q1, impact factor of 5-12) and more than 190 papers are in the Scopus index. In addition, he has published more than 80 papers in international conferences. He has a total citation more than 3000 and a h-index of 27 in Scopus (Author ID: 57195432490). He has a total citation of 4487 and a h-index of 30 in Google Scholar. He has been appointed as reviewer of high-impact (Q1) journals. He has also been appointed as editor of journals. He has received several awards. He owns one patent and two copyrights.

Nilofar Asim obtained her BSc in Applied Chemistry, MSc in Inorganic Chemistry from Tehran University and Ph.D. in Materials Science from National University of Malaysia. She is presently being an Associate professor at solar energy Research Institute, a center of excellence for the research and development in solar energy technology, National University of Malaysia (UKM). She has been involved in the field of materials science for more than 20 years. Her main contributions are in the synthesis of nanomaterials, composites, and investigation of their application; photocatalysts; geopolymers; materials related to a renewable energy application and recycling and valorization of waste materials for sustainability improvement.

Adnan Ibrahim, hold a Degree (Hons) in Manufacturing Systems Engineering from University of Portsmouth, United Kingdom, Master of Science in Integrated Product Development from University of Strat$_{hc}$lyde, United Kingdom and Doctor of Philosophy in Renewable Energy from Universiti Kebangsaan Malaysia. Currently he is involved with Advanced Solar Thermal Technology focusing on Nano Fluids & Nano Particles Storage Enhanced Photovoltaic Thermal (PV/T) Solar Collector System.